FXR1 promotes proliferation, invasion and migration of hepatocellular carcinoma *in vitro* and *in vivo*

KUN ZHAO[1-4], JIE GAO[1-4], JIHUA SHI[1-4], CHENGCHENG SHI[5], CHUN PANG[1-4], JIE LI[1-4], WENZHI GUO[1-4] and SHUIJUN ZHANG[1-4]

[1]Department of Hepatobiliary and Pancreatic Surgery; [2]Henan Diagnosis and Treatment League for Hepatopathy; [3]Henan Engineering and Research Center for Diagnosis and Treatment of Hepatobiliary and Pancreatic Surgical Diseases; [4]Henan Research Centre for Organ Transplantation; [5]Department of Pharmacy, The First Affiliated Hospital of Zhengzhou University, Zhengzhou, Henan 450052, P.R. China

Received March 2, 2022; Accepted October 7, 2022

DOI: 10.3892/ol.2022.13608

Abstract. Hepatocellular carcinoma (HCC) is a common malignancy that is associated with a poor prognosis. The extensively studied TGF-β pathway is mediated by SMAD proteins. FXR1, a protein-coding gene belonging to the fragile X-related (FXR) family, is involved in the TGF-β pathway. Previous studies have shown that FXR1 promotes the proliferation, invasion, and migration of colorectal cancer cells. The aim of the present study was to explore the effects of FXR1 on HCC via the TGF-β/SMAD signaling pathway. Immunohistochemical analysis was used to detect the expression of FXR1 in HCC and normal tissues. Western blotting was used to detect protein expression levels in the HCC cell lines, cell migration and invasion were assessed using Transwell assays, and cell proliferation was assessed using a colony formation assay. The ability of the liver cancer cells to grow *in vivo* was investigated using a nude mouse tumor-bearing model. The results showed that FXR1 expression was upregulated in HCC tissues compared with normal tissues. Knockdown of FXR1 resulted in reduced expression of SMAD2/3 and EMT-related proteins in HCC cells. In addition, FXR1 knockdown inhibited the proliferation, migration, and invasion of HCC cells. FXR1 knockdown also reversed the promoting effect of TGF-β on the invasive ability of HCC cells. Knockdown of SMAD2/3 reversed the increase in HCC cell invasion induced by FXR1 overexpression. Finally, upregulated FXR1 expression was associated with a poorer prognosis in patients with HCC. In conclusion, FXR1 promoted HCC proliferation, migration, and invasion through the regulation of SMAD2/3.

Correspondence to: Professor Shuijun Zhang, Department of Hepatobiliary and Pancreatic Surgery, The First Affiliated Hospital of Zhengzhou University, 1 East Jian She Road, Zhengzhou, Henan 450052, P.R. China
E-mail: zhangshuijun@zzu.edu.cn

Abbreviations: EMT, epithelial-mesenchymal transition; FXR, fragile X-related; GEPIA, gene expression profile interactive analysis platform; HCC, hepatocellular carcinoma; HRP, horseradish peroxidase; PPL, Public Protein/Plasmid Library; TGCA, The Cancer Genome Atlas; TGFBR1, TGF-β receptor complex type I; TGFBR2, TGF-β receptor complex type II

Key words: hepatocellular carcinoma, FXR1, SMAD2/3 pathway, migration, invasion, cancer

Introduction

Liver cancer is the third leading cause of cancer-related death and the sixth most commonly diagnosed cancer worldwide (1). Hepatocellular carcinoma (HCC) is the most common type of liver cancer. Viral hepatitis infection is a major risk factor for hepatocellular carcinoma in China (2,3). Despite advances in surgical techniques, procedural interventions, and the development of targeted drugs, the prognosis of HCC remains poor (4). Therefore, unraveling the pathogenesis of HCC and identifying novel and effective therapeutic targets have become the focus of current research (5-9).

FXR1 belongs to the fragile X-related (FXR) family (10,11); previous studies have shown that FXR1 can promote the proliferation, invasion, and migration of colorectal cancer cells (12). Moreover, FXR1 has been reported to play a role in the development of oral cancer and gliomas (13,14). However, the role and mechanism of FXR1 in HCC have not been elucidated.

In the early stages of tumor development, TGF-β inhibits tumor cell proliferation by inhibiting c-Myc, cyclin, and cyclin-dependent kinase activity, preventing the transition from the G1 to S phase. In the later stages of tumor development, TGF-β promotes tumor progression (15-17). The classical TGF-β pathway is mediated by SMAD proteins, which bind to type I and II TGF-β receptor complexes (TGFBR1 and TGFBR2), resulting in TGFBR phosphorylation and activation (11). TGFBR can further induce the phosphorylation of SMAD2/3, and the activated SMAD2/3 can further bind to SMAD4. Subsequently, the SMAD complex is transferred to the nucleus to exert its effects (18,19). One of the most critical processes that enable tumor cells to infiltrate and metastasize is epithelial-mesenchymal transition (EMT) (17,20). EMT causes epithelial cells to lose their epithelial phenotypes. It also

enhances tumor cell migration and invasion, anti-apoptotic processes, and extracellular matrix degradation (21,22).

In this study, we demonstrated that FXR1 knockdown led to a reduction in HCC cell migration and invasion, and it inhibited the stimulation of HCC cell migration and invasion via modulation of TGF-β. FXR1 overexpression in HCC cells promoted cell invasion, which was abrogated by inhibiting SMAD2/3.

Materials and methods

Cell culture. LM3 (cat. no. CL-0278), Huh7 (CL-0120), MHCC-97H (CL-0497) and Hep3B (cat. no. CL-0102) cells were purchased from Procell Life Science & Technology Co., Ltd. Cells were cultured in DMEM high glucose supplemented with 10% FBS, 100 mg/ml penicillin G, and 50 mg/ml streptomycin in a humidified incubator at 37˚C supplied with 5% CO_2. MHCC-97H (CL-0497) cells were used for western blotting.

Reagents and antibodies. TGF-β was purchased from PeproTech, Inc. FXR1 (cat. no. 67813-1-Ig, 1:10,00 or 1:100), Ki67 (27309-1-AP; 1:100) and β-actin (cat. no. 66009-1-Ig, 1:10,00) antibodies were purchased from ProteinTech Group, Inc. The FXR1 antibody was diluted 1:1,000 in the western blotting assay and 1:100 in immunohistochemistry assays. SMAD2/3 (cat. no. # 8685S, 1:1,000), N-Cadherin (cat. no. # 4061, 1:1,000), and slug (cat. no. 9585S, 1:1,000) antibodies were purchased from Cell Signaling Technology, Inc. The secondary antibodies used were HRP-conjugated Affinipure Goat Anti-Rabbit (1:2,000 or 1:50; cat. no. SA00001-2) and HRP-conjugated Affinipure Goat Anti-Mouse (1:2,000; cat. no. SA00001-1) (both from ProteinTech Group, Inc.). HRP-conjugated Affinipure Goat Anti-Rabbit was diluted 1:2,000 in the western blotting assay and 1:50 in immunohistochemistry assays. SMAD2/3 siRNA was purchased from Santa Cruz Biotechnology, Inc. (cat. no. sc-37238). shRNA was purchased from Public Protein/Plasmid Library. The sequences of the FXR1 knockdown shRNAs were: shFXR1#1, 5'-GCTAGAGGTTTCTTGGAATTT-3'; shFXR1#2, 5'-CGC CAGGTTCCATTTAATGAA-3'; and negative control (shNC), 5'-GTTCTCCGAACGTGTCACGTT-3'. The FXR1 expression plasmid with a 3'FLAG tag was purchased from Public Protein/Plasmid Library.

Reverse transcription-quantitative PCR. TRIzol® reagent was used to extract total RNA from tissues or cells, and 1 μg RNA was reverse transcribed to cDNA using a Vazyme reverse transcription kit according to the manufacturer's protocol (Vazyme Biotech Co., Ltd.; cat. no. R323-01). Amplification was performed using amplification reagent according to the manufacturer's protocol (Vazyme Biotech Co., Ltd.; cat. no. Q711-02). The thermocycling conditions for amplification were as follows: 95˚C for 5 min, followed by 40 cycles at 95˚C for 10 sec, 60˚C for 30 sec, and a final step at 95˚C for 15 sec, 60˚C for 60 sec and 95˚C for 15 sec. β-actin was used as the housekeeping gene. The sequences of the primers used for amplification were: β-actin forward, 5'-CATGTA CGTTGCTATCCAGGC-3' and reverse 5'-CTCCTTAATGTC ACGCACGAT-3'; SMAD2 forward, 5'-GATCCTAACAGA ACTTCCGCC-3' and reverse, 5'-CACTTGTTTCTCCATCTT CACTG-3'; and SMAD3 forward, 5'-TCCATCCCCGAAAAC ACTAAC-3' and reverse, 5'-CATCTTCACTCAGGTAGC CAG-3' (23). The relative expression level of the target genes was calculated using the $2^{-\Delta\Delta Cq}$ method (23).

Transfection. For transient transfection of plasmids, LM3 cells were transfected using Lipofectamine® 3000 (Thermo Fisher Scientific, Inc.). For transfection of shRNAs (final concentration, 30 μM), proliferating cells in a 6-well plate were incubated in serum-free DMEM containing Lipofectamine® 3000. After 4-6 h, the cells were incubated in supplemented DMEM for 48 h, and then treated with the newly configured puromycin (2 μg/ml) screening medium every day until no cell death was observed. The maintenance medium contained puromycin (2 μg/ml). To transfect siRNAs (final concentration, 20 μM), proliferating cells in a 6-well plate were incubated with serum-free DMEM supplemented with Lipofectamine® 3000. After 4-6 h, the cells were incubated in complete DMEM for 48 h and then selected with puromycin (2 μg/ml) until no cellular death was observed. The maintenance medium contained puromycin (2 μg/ml).

Western blotting. Total protein was extracted using RIPA lysis buffer supplemented with a mixture of PMSF, aprotinin, and phosphatase inhibitors. LM3 (cat. no. CL-0278), Huh7 (CL-0120), MHCC-97H (CL-0497) and Hep3B (cat. no. CL-0102) cells were used for western blotting. The protein concentration was measured using a Bicinchoninic protein assay (Thermo Fisher Scientific, Inc.). Proteins (30 μg per lane) were separated using SDS-PAGE on a 10% SDS gel, transferred to PVDF membranes, and incubated with the primary antibody, followed by incubation with the appropriate horseradish peroxidase (HRP)-conjugated secondary antibody at room temperature for 1 h. BeyoECL Plus (Beyotime Institute of Biotechnology) was used for signal visualization, and images were obtained using a Fushon Fx (Vilber Lourmat) imaging system.

Apoptosis evaluation using flow cytometry. A Beyotime Institute of Biotechnology apoptosis kit was used for testing (cat. no. C1069L). The cells were washed with PBS once and detached using pancreatic enzyme cell digestion solution, at room temperature until gentle aspiration with a pipette was sufficient to lift cells (ensuring over-digestion was avoided), after which the pancreatic enzyme cell digestion solution was removed. The cells were collected, mixed gently, and centrifuged at 1,000 x g at 4˚C for 5 min, after which the cells were collected and gently resuspend in PBS for counting. A total of 50-100 μl of the resuspended cell solution was taken, centrifuged at 1,000 x g at 4˚C for 5 min, the supernatant was discarded, 195 μl annexin V-mCherry Binding Buffer was added, and cells were gently resuspended. A total of 5 μl annexin V-mCherry was added and mixed gently, incubated at room temperature (20-25˚C) for 10-20 min, avoiding light, followed by incubation in an ice bath. Aluminum foil was used to protect against light. Cells were resuspended 2-3 times during incubation to ensure appropriate and equal staining. Subsequently, cells were analyzed using flow cytometry (BD FACSymphony™ A3; BD Biosciences) for Annexin V-mCherry red fluorescence (Beyotime Institute of

Biotechnology apoptosis kit; cat. no. C1069L). FlowJo™10 (BD Biosciences) was used for analysis.

Colony formation assay. After digestion of cells using cellular pancreatic enzyme during the logarithmic growth phase, cells were resuspended in supplemented media and counted. A total of 400-1,000 cells/well (generally 700 cells/well) were seeded in each experimental group in a 6-well culture plate and cultured for 14 days, changing the media every 3 days. After 14 days, 1 ml crystal violet dye solution was added to each well and incubated at room temperature for 10-20 min, after which cells were washed several times, dried, and imaged with a digital camera attached to a bright field microscope at a magnification of x200. Colonies consisting of ≥50 cells were counted.

Cell migration and invasion. Cell migration was determined using a Transwell assay. Transfected Hep3B or LM3 cells ($5x10^4$ per well) or cells treated with 20 ng/ml TGF-β were resuspended in 500 μl serum-free medium containing 2 μg/ml mitomycin C and added to the upper chamber to inhibit cell proliferation, and 500 μl supplemented media was added to the lower chamber. After incubation at 37˚C for 48 h, the cells on the upper surface of the filter membrane were removed using a swab and the filter membrane was incubated in 100% methanol at room temperature for 2 min. The cells that had migrated to the underside of the filter were stained with 0.5% crystal violet at room temperature for 20 min, and images were obtained using a bright field microscope. The number of cells that had migrated was counted using Image Pro Plus 6.0 (Media Cybernetics, Inc.). Cell invasion was determined using the same method as that for cell migration except cells were seeded in a Transwell chamber covered with Matrigel (BD Biosciences).

Mouse xenograft model. A total of 20 BALB/c nude mice were purchased from Beijing Vital River Laboratory Animal Technology Co., Ltd. Mice were maintained with a 12-h light/dark cycle under specific pathogen-free conditions. All animal experiments were approved by the Ethics Committee of the First Affiliated Hospital of Zhengzhou University (approval no. 2019-KY-21) and in accordance with the guidelines of the Office of Laboratory Animal Welfare. Mice were monitored daily and euthanized according to NIH-approved criteria for institutional humane endpoints if they failed to demonstrate a corrective response. For tumor growth experiments, stably transfected LM3 cells ($1x10^5$) were injected into mice by subcutaneous injection in the abdomen. The volume of the tumor was measured once every 2 days as follows: Volume=0.5x length x width x height; the total volume of each tumor did not exceed 4,400 mm^3. When the tumor size reached 12-20 mm the mice were euthanized via cervical dislocation; death was confirmed by lack of breathing and heartbeat.

Patients. The study included 88 patients with HCC (74 male and 14 female patients) treated at the First Affiliated Hospital of Zhengzhou University. HCC (2-3 cm) and normal tissue samples were obtained after surgery between January 2020 and December 2021. Patients were aged 30-76 years (median age, 56 years). Complete clinical information was available for included patients, and none of the patients had other malignancies or a history of chemotherapy or radiation therapy.

Immunohistochemical analysis. A total of 88 pairs of HCC and normal tissues (74 males and 14 female patients) were obtained from the First Affiliated Hospital of Zhengzhou University (Zhengzhou, China). The tumors of nude mice were tested for Ki67 after removal.

For immunohistochemistry, tissue sections were mounted on a glass slide, deparaffinized, and rehydrated. Samples were soaked in 100% alcohol, 100% alcohol, 95% alcohol, 75% alcohol and water for 5 min each for hydration. Heat-induced antigen retrieval was subsequently performed using 10 nmol/l citrate buffer (pH=6.0) for 10 min in a microwave oven (high heat). The slides were incubated with FXR1 (cat. no. 67813-1-Ig; 1:100) or Ki67 (27309-1-AP; 1:100) antibody overnight at 4˚C, followed by incubation with a HRP labeled secondary antibody (cat. no. SA00001-2; 1:50) at room temperature for 15 min. The slides were further stained with DAB developer and counterstained with 5% hematoxylin at room temperature for 3 min. Positive cells were stained brown.

The expression levels were scored based on the percentage of positive cells and the intensity of staining. The score was calculated as follows: 0, <5% positively stained cells; 1, 5-25% positively stained cells; 2, 25-50% positively stained cells; 3, 50-75% positively stained cells; and 4, >75% positively stained cells. The intensity was scored as follows: 0, negative staining; 1, light yellow staining; 2, brownish yellow staining; and 3, chocolate-brown staining. The final score was calculated by multiplying the percentage score by the intensity score. A score <8 was considered low, and a score ≥8, was considered high.

Bioinformatics analysis. The Oncomine online database (http://www.oncomine.org) was used to analyze FXR1 transcripts in HCC from the Rossher liver and Rossher liver 2 datasets. UALCAN (http://ualcan.path.uab.edu) was used to analyze the expression of FXR1 in HCC data from TCGA. GEPIA (http://gepia.cancer-pku.cn/) was used to analyze the correlations between i) FXR1 and SMAD2/3/4 mRNA levels and ii) FXR1 expression in TCGA. The threshold for mRNA levels was customized to allow for the stratification of subjects with low or high FXR1 mRNA levels. TCGA raw data, such as gene expression and clinicopathological data, were included in the UALCAN and cBioPortal analyses (http://www.cbioportal.org). Gene Set Enrichment Analysis (GSEA) was performed to explore potential biological pathways based on Kyoto Encyclopedia of Genes and Genomes (KEGG) gene sets using R software (version 4.1.2; https://www.r-project.org/). For KEGG enrichment analysis, the 'clusterProfiler' R package was used to decode potential targets downstream of FXR1, the gseKEGG function was used to explore the underlying biological significance. Based on gene count thresholds generated from the median value of FXR1 expression (TPM value=4.16), patients were classified into low and high groups.

Statistical analysis. SPSS software (version 22.0; IBM Corp.) was used for statistical analyses. A one-way ANOVA followed by a post hoc Bonferroni correction was used for the statistical analysis of mRNA expression, cell migration, and invasion. A Student's t-test was used to compare the differences between

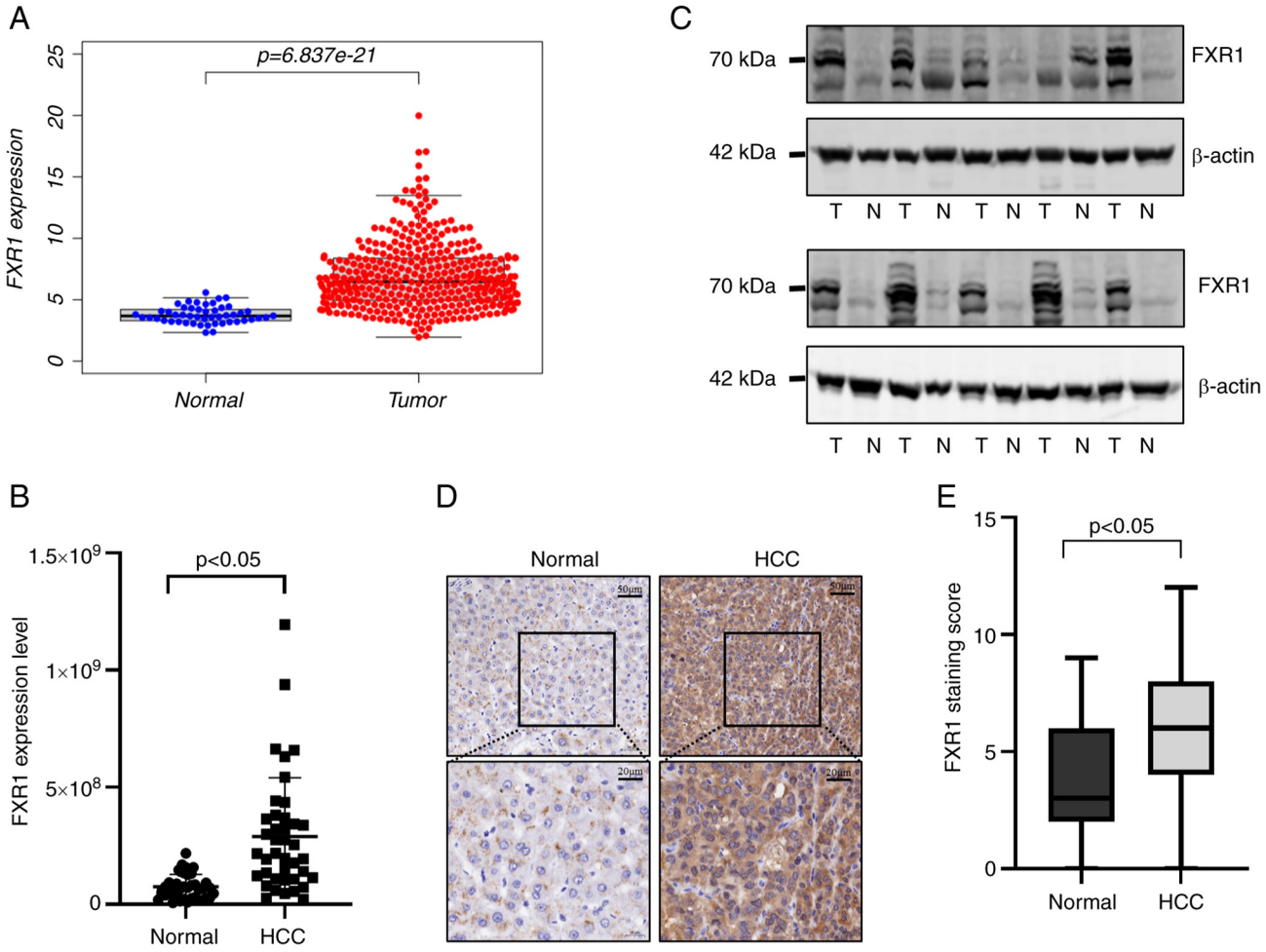

Figure 1. FXR1 is overexpressed in HCC. (A) Expression of FXR1 mRNA in HCC and normal tissues. (B) FXR1 proteomic expression in HCC and normal tissues. (C) Expression of FXR1 protein in HCC tissues. (D) Immunohistochemical analysis of FXR1 expression in HCC and normal tissues. (E) Box plot of FXR1 expression in HCC and normal tissues. FXR1, fragile X-related 1; HCC, hepatocellular carcinoma.

two groups. A Pearson's correlation test was used to assess correlations. Paired samples were tested using a paired t-test. P<0.05 was considered to indicate a statistically significant difference.

Results

FXR1 expression is upregulated in HCC. To investigate FXR1 expression in HCC, data from the HCC cohort in TCGA was used; FXR1 was upregulated in HCC (Fig. 1A). Validation of FXR1 expression was also performed using HCC and normal tissues, and the results showed that FXR1 was highly expressed in HCC at the protein level (Fig. 1B and C). Next, FXR1 expression was assessed in HCC and normal tissues using immunohistochemical microarrays, and similar results were observed; FXR1 expression was higher in HCC tissues than in normal tissues (Fig. 1D and E).

FXR1 is positively associated with SMAD2/3/ in HCC cells. To explore potential targets downstream of FXR1, GSEA was used to identify the latent biological pathways based on KEGG gene sets; the top 10 corresponding genes are shown in Fig. 2A. Bioinformatics analysis was used to assess the correlation between FXR1 and genes from TCGA. The mRNA expression levels of FXR1 were positively correlated with the mRNA expression levels of SMAD2/3 (Fig. 2B).

FXR1 promotes slug/N-cadherin expression and TGF-β-induced HCC cell migration and invasion. We further investigated the effects of FXR1 on the migratory and invasive effects of HCC and the involvement of SMAD2/3. The protein expression levels of FXR1 in five different HCC cell lines were examined, and the results showed that FXR1 was relatively highly expressed in LM3 and Hep3B cells (Fig. 3A). shRNAs were used to knock down FXR1 expression in LM3 and Hep3B cells, and knockdown was confirmed using western blotting (Fig. 3B). Western blotting also showed a decrease in the expression of N-cadherin and Slug in FXR1 knockdown cells (Fig. 3B). These results suggest that FXR1 affects the expression of EMT-related proteins. In addition, the expression levels of SMAD2/3 decreased upon FXR1 knockdown (Fig. 3B).

TGF-β promotes tumor migration and invasion through EMT (24,25). The effect of FXR1 on the TGF-β-induced migration and invasion in HCC cells was thus next assessed. FXR1 knockdown cells transfected with the two different shRNAs consistently inhibited the migration and invasion of LM3 and Hep3B cells (Fig. 3C and D). Additionally, shRNA-induced

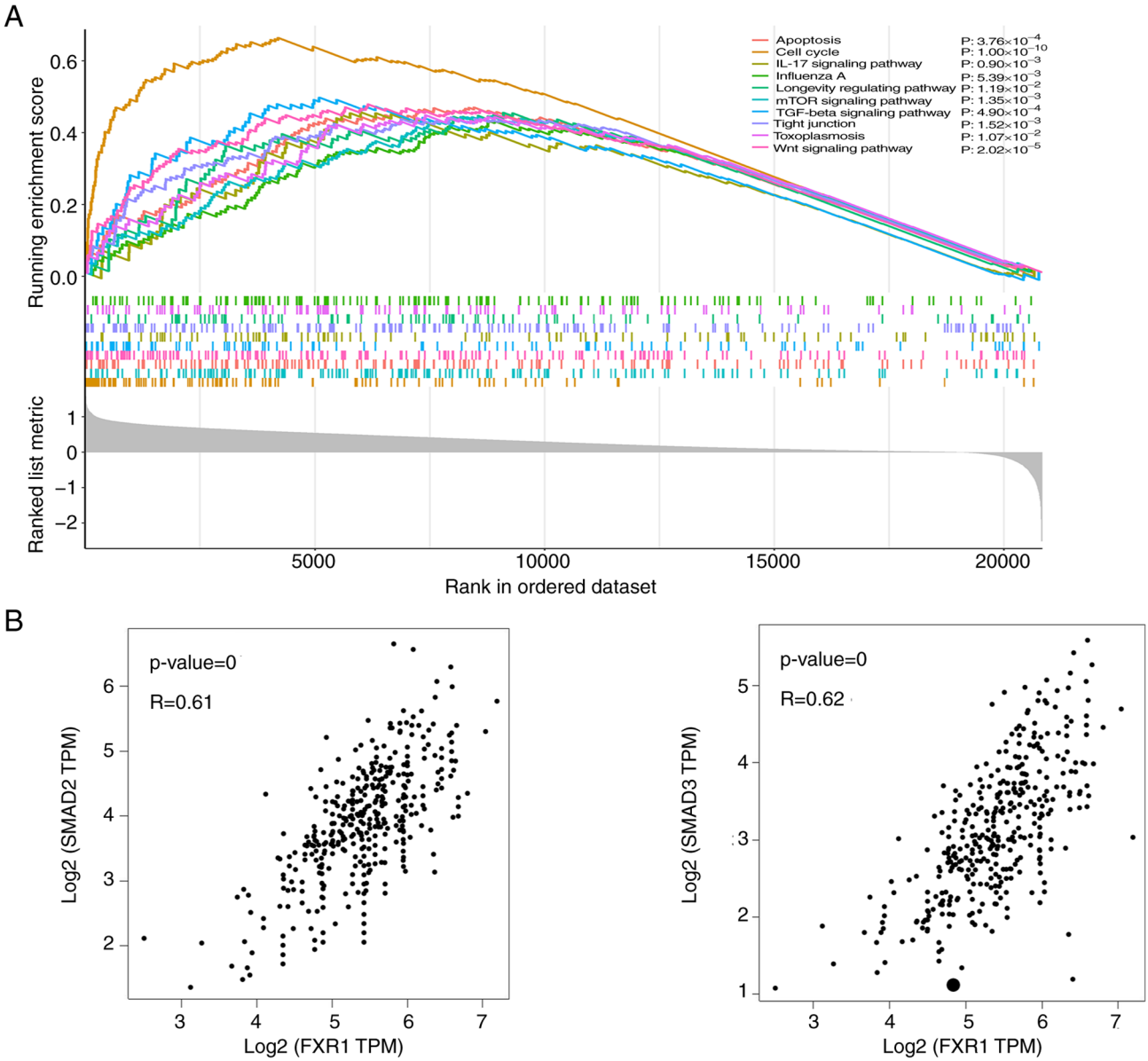

Figure 2. Exploration of the underlying biological function and correlation analysis between FXR1 and SMAD2/3. (A) GSEA showed the potentially associated biological pathways based on KEGG gene sets (left), and the top 10 corresponding genes (right). (B) Correlation scatter plot of FXR1 and SMAD2/3. Gene expression levels are represented as $\log_2$[TPM]. FXR1, fragile X-related 1; HCC, hepatocellular carcinoma; TPM, transcripts per million.

FXR1 knockdown inhibited the TGF-β-induced increase in HCC cell migration and invasion when compared with cells treated with TGF-β and transfected with shNC (Fig. 3C and D).

Knockdown of FXR1 inhibits the proliferation of HCC cells and promotes early apoptosis of HCC cells. To validate the effect of FXR1 on apoptosis in HCC cells, two different shRNAs were used to knockdown FXR1 in Hep3B and LM3 cells, and apoptosis was assessed using flow cytometry. The results showed that FXR1 knockdown enhanced early apoptosis in HCC cells (Fig. 4A and B). Additionally, the knockdown of FXR1 inhibited the proliferation of HCC cells in the colony formation assay. These results were validated in both Hep3B and LM3 cells (Fig. 4C and D). These results suggest that knockdown of FXR1 inhibited the proliferation of HCC cells and promoted early apoptosis of HCC cells.

Knockdown of SMAD2/3 inhibits the FXR1-induced increase in LM3 cell invasion. FXR1 overexpressing LM3 cell lines with or without SMAD2/3 knockdown were established. RT-qPCR was used to verify the knockdown efficiency of siSMAD2/3 (Fig. S1). The results showed that FXR1 overexpression enhanced LM3 cell invasion. Knockdown of SMAD2/3 inhibited the FXR1 overexpression-induced increase in the invasion of LM3 cells (Fig. 5B). The transfection efficiency of FXR1 and SMAD2/3 was verified using western blotting (Fig. 5A). The results of this experiment validated the role of SMAD2/3 in the FXR1-induced increase in HCC invasion.

FXR1 knockdown inhibits the growth of LM3 cells in vivo. To verify the role of FXR1 *in vivo*, mice were injected with shNC-transfected LM3 cells or shFXR1-transfected LM3 cells. By measuring the volume of the tumors every 2 days, the results showed that tumors grew slower in FXR1 knockdown

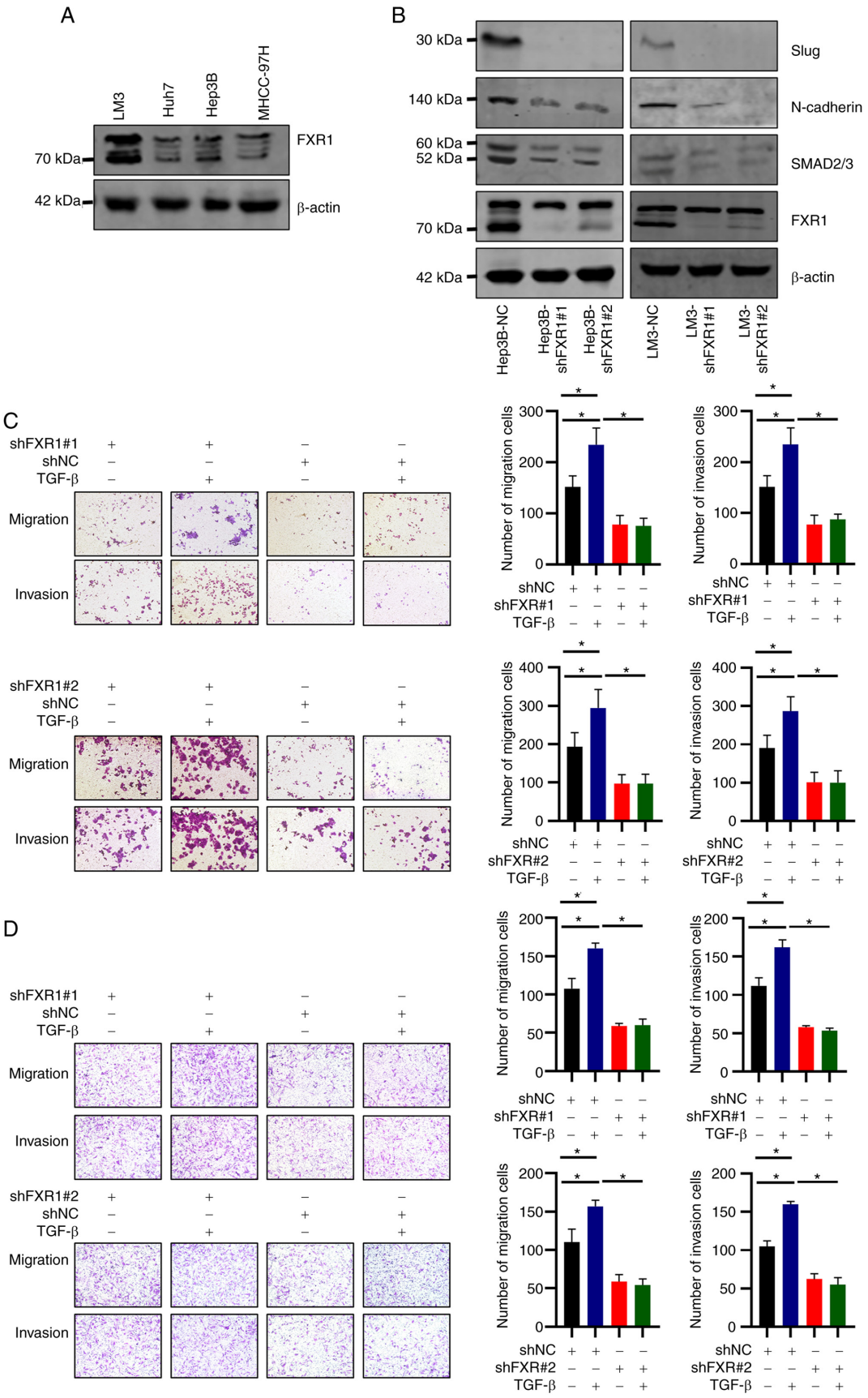

Figure 3. FXR1 promotes slug/N-cadherin expression and TGF-β-induced HCC cell migration and invasion. (A) FXR1 expression in HCC cells. (B) Hep3B and LM3 cells were transfected with shNC, shFXR1#1, or shFXR1#2, and western blotting was used to determine knockdown efficiency. (C) Hep3B and (D) LM3 cells were transfected with shNC, shFXR1#1, or shFXR1#2, and treated with or without TGF-β, followed by cell migration and invasion assays. The cells were then observed microscopically (magnification, x200). The relative cell migration or invasion was plotted. Cell migration or invasion was normalized to the shNC-transfected and TGF-β-untreated group as appropriate. Note: The difference in cell status and the time of spreading the plates resulted in inconsistencies in the number of cells in the control group at different times. Data are presented as the mean ± SD of three repeats. *P<0.05. FXR1, fragile X-related 1; HCC, hepatocellular carcinoma; sh, short hairpin; NC, negative control.

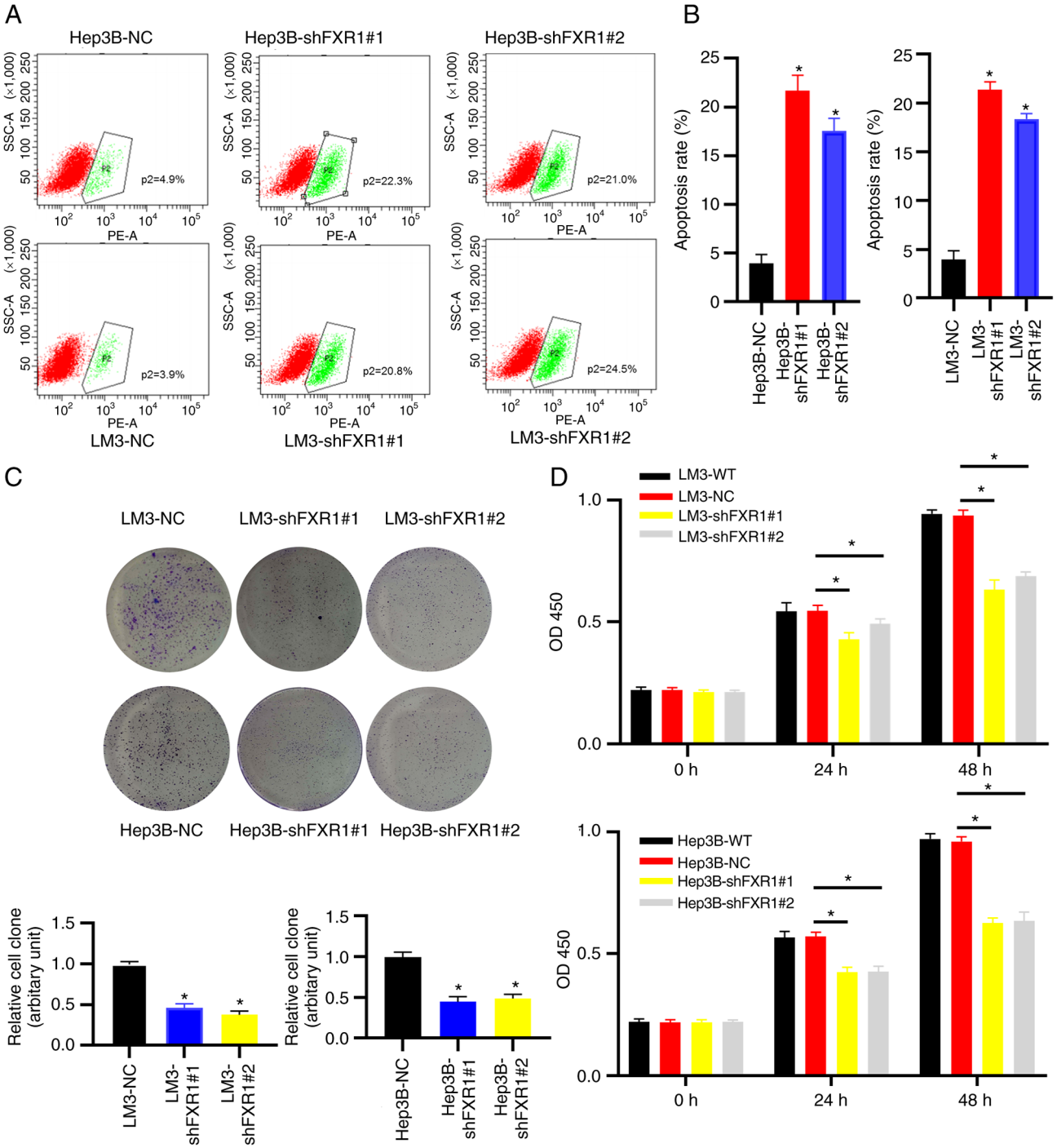

Figure 4. Knockdown of FXR1 inhibits the proliferation of HCC cells and promotes early apoptosis of HCC cells. (A) Hep3B and LM3 cells were transfected with shNC, shFXR1#1 or shFXR1#2, followed by flow cytometry analysis. (B) Flow cytometry analysis of apoptosis. (C) Hep3B and LM3 cells were transfected with shNC, shFXR1#1 or shFXR1#2, followed by colony formation assays and imaging with a digital camera attached to a bright field microscope at a magnification of x200. (D) Hep3B and LM3 cells were transfected with shNC, shFXR1#1, or shFXR1#2, followed by CCK-8 assays. *P<0.05. FXR1, fragile X-related 1; NC, negative control; WT, wild-type.

cells (Fig. 6A and B). The average diameter of the NC tumors was 14.5 mm (range, 12.66-16.84 mm) and the mean diameter of the shFXR1 tumors was 11.9 mm (range, 9.15-14.70 mm); the difference was statistically significant. The expression of Ki67 in the tumors was assessed using immunohistochemistry, which showed a significant decrease in Ki67 expression in the tumors after FXR1 knockdown (Fig. 6C and D). These data indicate that FXR1 knockdown inhibits HCC proliferation *in vivo*.

Discussion

FXR1 belongs to the FXR protein family. The results of the present study indicated that FXR1 expression was upregulated in HCC tissues. Knockdown of FXR1 inhibited the malignant behavior of HCC cells. Specifically, FXR1 knockdown effectively inhibited the migratory and invasive abilities of HCC cells. FXR1 knockdown also inhibited the proliferation of HCC cells. Furthermore, FXR1 knockdown increased early

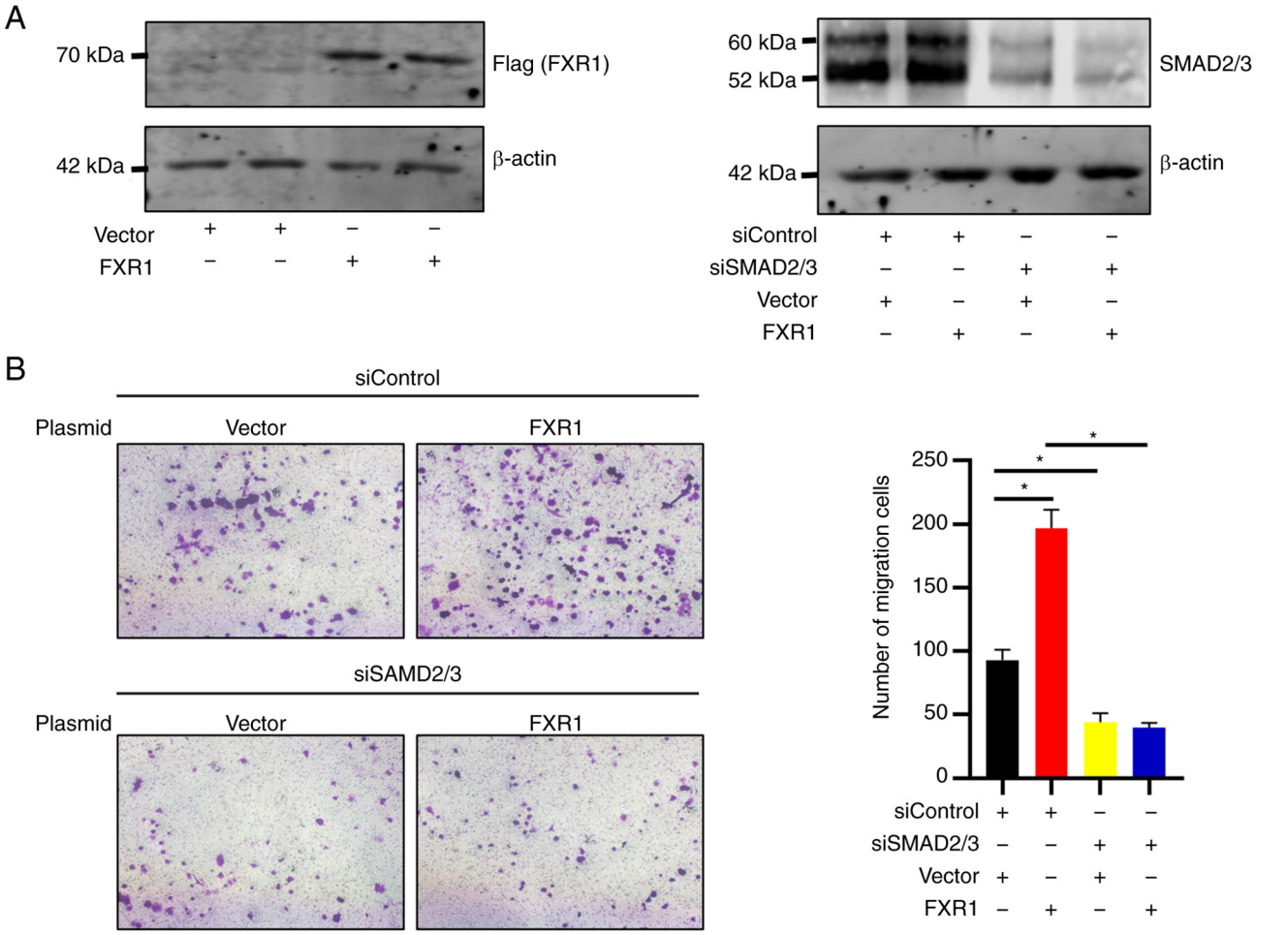

Figure 5. Effects of FXR1 overexpression and SMAD2 knockdown on LM3 invasion. (A) FXR1 and SMAD2/3 expression after transfection was verified by western blotting. (B) LM3 cells were transfected with empty vector or FLAG-tagged FXR1 expression plasmid, and siControl or siSAMD2/3, followed by cell invasion assays and imaging with a digital camera attached to a bright field microscope at a magnification of x200. *P<0.05. FXR1, fragile X-related 1; si, small interfering.

apoptosis of HCC cells. Using bioinformatic analysis, it was shown that patients with high FXR1 expression had a worse prognosis. These results suggested that FXR1 functions as an oncogene in HCC. This finding is consistent with the role of FXR1 in other tumors. In prostate cancer, FXR1 downregulation is associated with the inhibition of cell proliferation, decreased cell viability, and impaired migration and invasion of prostate cancer cells (26). FXR1 is highly expressed in gliomas, and the knockdown of FXR1 leads to the inhibition of the malignant biological behaviors of glioma cells (9). In colorectal cancer, FXR1 acts as an oncogene that increases the proliferation, migration, and invasion of cancer cells (12).

Bioinformatics is an important tool that is increasingly being used as an initial approach to identify relevant target proteins (27-29). Bioinformatics analysis was used in the present study to screen SMAD2/3 as a target of the downstream action of FXR1. TGF-β-SMAD signaling promotes the development of EMT and the metastasis of HCC (30,31). The best-known SMAD3 targets are EMT-related genes such as slug (32). EMT is closely associated with cancer metastasis (33-35), and can be induced by environmental stresses (such as inflammation, reactive oxygen species, hypoxia, hypoxia/reoxygenation), and certain extracellular mediators (including TGF-β, fibroblast growth factor-2, and epidermal growth factor) (36). The EMT-related proteins slug and N-cadherin, play a significant role in invasive metastasis. In the present study, western blotting was used to preliminarily validate the expression of proteins downstream of FXR1. The results showed that the knockdown of FXR1 inhibited the expression of SMAD2/3, whereas knockdown of SMAD2/3 suppressed the expression of EMT-related proteins.

TGF-β was selected for analysis in this preliminary study as it is a well-established pathway; additional pathways will be investigated in future research. The Smad pathway is known to be a major transducer of TGF-β signaling and is important in TGF-β-induced EMT (37). TGF-β plays a complex double-edged role in tumors. Early in tumorigenesis, TGF-β acts as a tumor suppressor through broad multicellular inhibition; however, after tumor formation, it acts as a pro-proliferative agent (38,39). In HCC, TGF-β plays a key role in coordinating and regulating the corresponding phenotype in HCC (40). GSEA showed the latent biological pathways based on KEGG gene sets. The TGF-β pathway was thus chosen as the primary research target in this study. TGF-β signaling in hepatocytes is associated with liver fibrosis and carcinogenesis (41). SMAD2/3 is a key molecule in the TGF-β

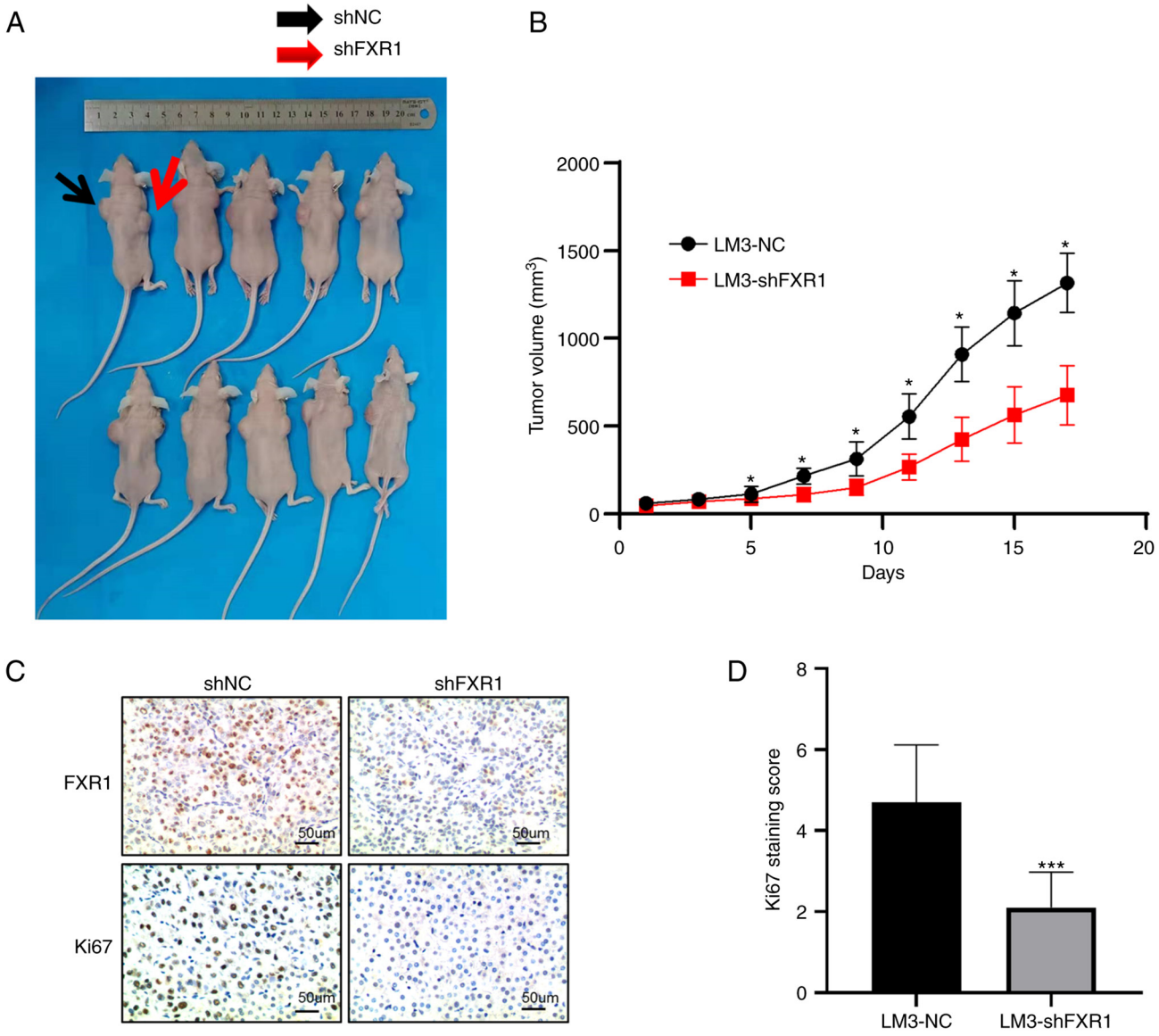

Figure 6. FXR1 knockdown inhibits the growth of LM3 cells *in vivo*. (A and B) Nude mice were injected with shNC or shFXR1-transfected LM3 cells. Tumor volume growth was slower after the knockdown of FXR1 than in the control mice. (C and D) Ki67 expression in the tumors was assessed using immunohistochemistry. *P<0.05, ***P<0.001 vs. LM3-NC group. FXR1, fragile X-related 1; sh, short hairpin; NC, negative control.

pathway. As a transcription factor, SMAD2/3 can positively or negatively regulate the expression of several genes (42,43). The promotion of HCC cell migration and invasion by TGF-β was confirmed in this study. FXR1 knockdown eliminated TGF-β-induced migration and invasion of HCC cells. Conversely, the promotion of HCC cell invasion by FXR1 overexpression could be inhibited by SMAD2/3 knockdown. These data suggest that SMAD2/3 is at least partially involved in the FXR1-mediated increase in HCC cell invasion. However, the specific regulatory mechanism by which FXR1 modulates SMAD2/3 mRNA expression is unknown.

A nude mouse xenograft model was used to explore the effects of FXR1 *in vivo*. Tumor Ki-67 protein expression is associated with a poor prognosis (44,45). The results of the present study showed that FXR1 knockdown inhibited tumor growth in nude mice. Moreover, immunohistochemistry analysis showed a significant decrease in Ki67 expression in tumors following FXR1 knockdown. This finding suggests that FXR1 influences HCC cell proliferation *in vivo*. In addition to classical SMAD signaling, TGF-β can also trigger non-classical kinase cascades, leading to the activation of other signaling pathways, such as PI3K, MAPK, and mTOR, which play an important role in tumorigenesis (46-48). Other mechanisms by which FXR1 promotes malignant behaviors in HCC need to be further explored. Further studies are required to verify whether FXR1 is a potential target for HCC therapy.

Since the present study did not directly confirm the relationship between FXR1 and the SMAD pathway, instead only showing an indirect relationship, further studies are required to assess this.

In conclusion, the present study is the first to show that aberrant FXR1 expression in HCC may promote the malignant biological behavior of HCC cells. Upregulated FXR1 expression is indicative of a poorer prognosis in HCC. In addition, SMAD2/3 was at least partially involved in the FXR1-mediated

increase in HCC cell invasion. Thus, FXR1 may serve as a novel therapeutic target for the management of HCC.

Acknowledgements

Not applicable.

Funding

This work was funded by Henan Provincial Ministry of Medical Science and Technology Research Youth Project (grant no. SBGJ202103061) and the National Natural Science Foundation of China (grant no. 82103282).

Availability of data and materials

The datasets used and/or analyzed during the current study are available from the corresponding author on reasonable request.

Authors' contributions

All of the authors have seen and confirmed the authenticity of the raw data generated during the study. KZ, JG, JS, CS, CP, JL, WG and SZ conceived and designed the study. KZ, JG and JS performed the experiments and analyzed the data. JG and SZ revised the manuscript. All authors read and approved the final manuscript.

Ethics approval and consent to participate

Written informed consent was obtained from patients (or their parents/guardians) prior to enrollment in this study. Ethical approval for the use of human/human tissues was obtained from the Ethics Committee of the First Affiliated Hospital of Zhengzhou University where the experiments were conducted prior to the commencement of the study. This study was approved by the Ethics Committee of the First Affiliated Hospital of Zhengzhou University (approval no. 2019-KY-21).

Patient consent for publication

Not applicable.

Competing interests

The authors declare that they have no competing interests.

References

1. Sung H, Ferlay J, Siegel RL, Laversanne M, Soerjomataram I, Jemal A and Bray F: Global cancer statistics 2020: GLOBOCAN estimates of incidence and mortality worldwide for 36 cancers in 185 countries. CA Cancer J Clin 71: 209-249, 2021.
2. Xie Y: Hepatitis B virus-associated hepatocellular carcinoma. Adv Exp Med Biol 1018: 11-21, 2017.
3. Jiang Y, Han QJ and Zhang J: Hepatocellular carcinoma: Mechanisms of progression and immunotherapy. World J Gastroenterol 25: 3151-3167, 2019.
4. Piñero F, Dirchwolf M and Pessôa MG: Biomarkers in hepatocellular carcinoma: Diagnosis, prognosis and treatment response assessment. Cells 9: 1370, 2020.
5. Dimri M and Satyanarayana A: Molecular signaling pathways and therapeutic targets in hepatocellular carcinoma. Cancers (Basel) 12: 491, 2020.
6. Akula SM, Abrams SL, Steelman LS, Emma MR, Augello G, Cusimano A, Azzolina A, Montalto G, Cervello M and McCubrey JA: RAS/RAF/MEK/ERK, PI3K/PTEN/AKT/mTORC1 and TP53 pathways and regulatory miRs as therapeutic targets in hepatocellular carcinoma. Expert Opin Ther Targets 23: 915-929, 2019.
7. Fujiwara N, Friedman SL, Goossens N and Hoshida Y: Risk factors and prevention of hepatocellular carcinoma in the era of precision medicine. J Hepatol 68: 526-549, 2018.
8. Xing R, Gao J, Cui Q and Wang Q: Strategies to improve the antitumor effect of immunotherapy for hepatocellular carcinoma. Front Immunol 12: 783236, 2021.
9. Chen Y, Li L, Lan J, Cui Y, Rao X, Zhao J, Xing T, Ju G, Song G, Lou J and Liang J: CRISPR screens uncover protective effect of PSTK as a regulator of chemotherapy-induced ferroptosis in hepatocellular carcinoma. Mol Cancer 21: 11, 2022.
10. Hoogeveen AT, Willemsen R and Oostra BA: Fragile X syndrome, the Fragile X related proteins, and animal models. Micros Res Tech 57: 148-155, 2002.
11. Majumder M, Johnson RH and Palanisamy V: Fragile X-related protein family: A double-edged sword in neurodevelopmental disorders and cancer. Crit Rev Biochem Mol Biol 55: 409-424, 2020.
12. Jin X, Zhai B, Fang T, Guo X and Xu L: FXR1 is elevated in colorectal cancer and acts as an oncogene. Tumour Biol 37: 2683-2690, 2016.
13. Majumder M and Palanisamy V: RNA binding protein FXR1-miR301a-3p axis contributes to p21WAF1 degradation in oral cancer. PLoS Genet 16: e1008580, 2020.
14. Cao S, Zheng J, Liu X, Liu Y, Ruan X, Ma J, Liu L, Wang D, Yang C, Cai H, *et al*: FXR1 promotes the malignant biological behavior of glioma cells via stabilizing MIR17HG. J Exp Clin Cancer Res 38: 37, 2019.
15. Zhao M, Mishra L and Deng CX: The role of TGF-β/SMAD4 signaling in cancer. Int J Biol Sci 14: 111-123, 2018.
16. Colak S and Ten Dijke P: Targeting TGF-β signaling in cancer. Trends Cancer 3: 56-71, 2017.
17. Hao Y, Baker D and Ten Dijke P: TGF-β-mediated epithelial-mesenchymal transition and cancer metastasis. Int J Mol Sci 20: 2767, 2019.
18. Hu HH, Chen DQ, Wang YN, Feng YL, Cao G, Vaziri ND and Zhao YY: New insights into TGF-β/Smad signaling in tissue fibrosis. Chem Biol Interact 292: 76-83, 2018.
19. Aashaq S, Batool A, Mir SA, Beigh MA, Andrabi KI and Shah ZA: TGF-β signaling: A recap of SMAD-independent and SMAD-dependent pathways. J Cell Physiol 237: 59-85, 2021.
20. Pallasch FB and Schumacher U: Angiotensin Inhibition, TGF-β and EMT in Cancer. Cancers (Basel) 12: 2785, 2020.
21. Suarez-Carmona M, Lesage J, Cataldo D and Gilles C: EMT and inflammation: Inseparable actors of cancer progression. Mol Oncol 11: 805-823, 2017.
22. Babaei G, Aziz SG and Jaghi NZZ: EMT, cancer stem cells and autophagy; The three main axes of metastasis. Biomed Pharmacother 133: 110909, 2021.
23. Livak KJ and Schmittgen TD: Analysis of relative gene expression data using real-time quantitative PCR and the 2(-Delta Delta C(T)) method. Methods 25: 402-408, 2001.
24. Syed V: TGF-β signaling in cancer. J Cell Biochem 117: 1279-1287, 2016.
25. Zhang K, Fang T, Shao Y and Wu Y: TGF-β-MTA1-SMAD7-SMAD3-SOX4-EZH2 signaling axis promotes viability, migration, invasion and EMT of hepatocellular carcinoma cells. Cancer Manag Res 13: 7087-7099, 2021.
26. Cao H, Gao R, Yu C, Chen L and Feng Y: The RNA-binding protein FXR1 modulates prostate cancer progression by regulating FBXO4. Funct Integr Genomics 19: 487-496, 2019.
27. Li K, Du Y, Li L and Wei DQ: Bioinformatics approaches for anti-cancer drug discovery. Curr Drug Targets 21: 3-17, 2020.
28. Anashkina AA, Leberfarb EY and Orlov YL: Recent trends in cancer genomics and bioinformatics tools development. Int J Mol Sci 22: 12146, 2021.
29. Tsimberidou AM: Targeted therapy in cancer. Cancer Chemother Pharmacol 76: 1113-1132, 2015.
30. Yoshida K, Murata M, Yamaguchi T, Matsuzaki K and Okazaki K: Reversible human TGF-β signal shifting between tumor suppression and fibro-carcinogenesis: Implications of smad phospho-isoforms for hepatic epithelial-mesenchymal transitions. J Clin Med 5: 7, 2016.
31. Fransvea E, Angelotti U, Antonaci S and Giannelli G: Blocking transforming growth factor-beta up-regulates E-cadherin and reduces migration and invasion of hepatocellular carcinoma cells. Hepatology 47: 1557-1566, 2008.

32. Bai X, Yi M, Jiao Y, Chu Q and Wu K: Blocking TGF-β signaling to enhance the efficacy of immune checkpoint inhibitor. Onco Targets Ther 12: 9527-9538, 2019.
33. Pastushenko I and Blanpain C: EMT transition states during tumor progression and metastasis. Trends Cell Biol 29: 212-226, 2019.
34. Bakir B, Chiarella AM, Pitarresi JR and Rustgi AK: EMT, MET, plasticity, and tumor metastasis. Trends Cell Biol 30: 764-776, 2020.
35. Lu W and Kang Y: Epithelial-mesenchymal plasticity in cancer progression and metastasis. Dev Cell 49: 361-374, 2019.
36. Yuan GJ, Li QW, Shan SL, Wang WM, Jiang S and Xu XM: Hyperthermia inhibits hypoxia-induced epithelial-mesenchymal transition in HepG2 hepatocellular carcinoma cells. World J Gastroenterol 18: 4781-4786, 2012.
37. Kimura-Tsuchiya R, Ishikawa T, Kokura S, Mizushima K, Adachi S, Okajima M, Matsuyama T, Okayama T, Sakamoto N, Katada K, *et al*: The inhibitory effect of heat treatment against epithelial-mesenchymal transition (EMT) in human pancreatic adenocarcinoma cell lines. J Clin Biochem Nutr 55: 56-61, 2014.
38. Wang J, Xu Z, Wang Z, Du G and Lun L: TGF-beta signaling in cancer radiotherapy. Cytokine 148: 155709, 2021.
39. Zhang M, Zhang YY, Chen Y, Wang J, Wang Q and Lu H: TGF-β signaling and resistance to cancer therapy. Front Cell Dev Biol 9: 786728, 2021.
40. Li H, He G, Yao H, Song L, Zeng L, Peng X, Rosol TJ and Deng X: TGF-β induces degradation of PTHrP through ubiquitin-proteasome system in hepatocellular carcinoma. J Cancer 6: 511-518, 2015.
41. Suwa K, Yamaguchi T, Yoshida K, Murata M, Ichimura M, Tsuneyama K, Seki T and Okazaki K: Smad phospho-isoforms for hepatocellular carcinoma risk assessment in patients with nonalcoholic steatohepatitis. Cancers (Basel) 12: 286, 2020.
42. Yoshida K, Matsuzaki K, Murata M, Yamaguchi T, Suwa K and Okazaki K: Clinico-pathological importance of TGF-β/phospho-smad signaling during human hepatic fibrocarcinogenesis. Cancers (Basel) 10: 183, 2018.
43. Kaminska B, Wesolowska A and Danilkiewicz M: TGF beta signalling and its role in tumour pathogenesis. Acta Biochim Pol 52: 329-337, 2005.
44. Burkhart RA, Ronnekleiv-Kelly SM and Pawlik TM: Personalized therapy in hepatocellular carcinoma: Molecular markers of prognosis and therapeutic response. Surg Oncol 26: 138-145, 2017.
45. Qin LX and Tang ZY: The prognostic molecular markers in hepatocellular carcinoma. World J Gastroenterol 8: 385-392, 2002.
46. Stefani C, Miricescu D, Stanescu S II, Nica RI, Greabu M, Totan AR and Jinga M: Growth factors, PI3K/AKT/mTOR and MAPK signaling pathways in colorectal cancer pathogenesis: Where are we now? Int J Mol Sci 22: 10260, 2021.
47. Shorning BY, Dass MS, Smalley MJ and Pearson HB: The PI3K-AKT-mTOR pathway and prostate cancer: At the crossroads of AR, MAPK, and WNT signaling. Int J Mol Sci 21: 4507, 2020.
48. Kumari N, Reabroi S and North BJ: Unraveling the molecular nexus between GPCRs, ERS, and EMT. Mediators Inflamm 2021: 6655417, 2021.